Entrapment of PMMA Polymer Strands in Micro- and Mesoporous Materials

Karin Moller,*,† Thomas Bein,† and Reinhard X. Fischer‡

Department of Chemistry, Purdue University, West Lafayette, Indiana 47907, and Fachbereich Geowissenschaften, Universität Bremen, D-28359 Bremen, Germany

Received January 13, 1998. Revised Manuscript Received April 29, 1998

The synthesis of host−guest composites consisting of entrapped strands of poly(methylmethacrylate) (PMMA) within the pores of inorganic hosts is described. Methyl methacrylate was adsorbed into microporous hosts including zeolite NaY, mordenite, beta, and ZSM-5 and then polymerized. Adsorption and polymerization was also performed in the mesoporous materials MCM-41 and MCM-48. The adsorption of methyl methacrylate (MMA) and its conversion to PMMA was followed by FTIR spectroscopy. Nitrogen sorption isotherms confirm the filling of the micro- and mesopores with the polymer. Thermogravimetry (TGA) shows that the polymer content of the composites increases with increasing pore volume, while no polymer deposition on the external host surface is detected with scanning and transmission electron microscopy. The polymers confined in the 6−35 Å diameter channels of the hosts do not show characteristic bulk behavior with respect to their glass transition temperature.

Introduction

The quest to create ever new materials with optimized, predetermined characteristics has spurred an increasing interest in hybrid materials. It has been found that, by combining inorganic and organic components either at the molecular level or in their partially condensed forms, the mechanical, chemical, or physical properties of these composites can be controlled intelligently over wide ranges.[1] These properties are highly influenced by the nature of the constituents as well as the reaction pathway chosen for their preparation. In general, interactions between the inorganic and organic components of the composite can range from weak forces such as hydrogen bonding to strong covalent bonds. An intoduction to the chemistry of hybrid formation and a review of this area has recently been published by Judeinstein and Sanchez.[2] The most traditional approach leading to composite materials is the mixing of inorganic and organic components. Advanced sol−gel techniques include the in situ condensation of metal oxides in a polymer matrix. For example, the mechanical properties of poly(methyl methacrylate) (PMMA) were greatly improved by condensation of tetraethoxysilane (TEOS) within solutions of the polymer.[3,4] Another approach leading to composites is to use a single modified silicon alkoxide precursor such as $Si(OR)_4$ where the OR groups are all hydrolizable. Condensation and polymerization of the siliceous and organic components thus leads to the hybrid materials. Composites with covalent bonding between the two constituents can be formed with alkoxides containing 2−3 reactive −OR and 1−2 nonlabile functional groups R′ in precursors of composition $R'_xSi(OR)_{4-x}$.

In this paper we report the synthesis of composites of micro- and mesoporous hosts with encapsulated PMMA. Usually, silicate fillers are reacted with silane-coupling agents to improve miscibility and chemical bonding. An elegant approach for the grafting of PMMA was reported by Schouten et al.,[5] who functionalized aerosil particles with an amino-functional silane-coupling agent which in turn was used to covalently anchor the initiator for the final polymerization of MMA. However, for certain purposes, e.g., applications in aqueous environments, these materials might be subject to hydrolytic degradation. Alternatively, by forming interpenetrating systems, one might enhance the stability of the composite. Thus, using porous silicates allows a penetration of polymers into the inorganic phase. For example, sol−gel-derived monoliths with pores of 160 Å mean diameter were used by Pope et al.[6] They impregnated the support with MMA that was subsequently polymerized, resulting in transparent composites. By changing the composition, properties such as density, refractive index, or hardness could be modified. Porous glass slabs with smaller mean pore sizes (44 Å) were used by King et al. to prepare PMMA composites.[7]

Layered hosts, such as metal chalcogenides, phosphates, oxychlorides, or layered silicates, have been used

* To whom correspondence should be addressed.
† Purdue University.
‡ Universität Bremen.

(1) Mark, J. E.; Lee, C. Y.-C; Bianconi, P. A. *Hybrid Organic−Inorganic Composites*; ACS Symposium Series 585; American Chemical Society: Washington, DC, 1995.
(2) Judeinstein, P.; Sanchez, C. *J. Mater. Chem.* **1996**, *6*, 511.
(3) Landry, C. J. T.; Coltrain, B. K.; Wesson, J. A.; Zumbulyadis, N.; Lippert, J. L. *Polymer* **1992**, *33*, 1498.
(4) Rodrigues, D. E.; Risch, B. G.; Wilkes, G. L. *Chem. Mater.* **1997**, *9*, 2709.
(5) Boven, G. B.; Osterling, M. L. C. M.; Challa, G.; Schouten, A. J. *Polymer* **1990**, *31*, 2377.
(6) Pope, E. J. A.; Asami, M.; Meckenzie, J. D. *J. Mater. Res.* **1989**, *4*, 1018.
(7) Li, X.; King, T.; Pallikari-Viras, F. *J. Non-Cryst. Solids* **1994**, *170*, 243.

S0897-4756(98)00020-9 CCC: $15.00
Published on Web 06/26/1998

successfully to enhance the mechanical and thermal performance of hybrid nanocomposites. The interlayer distance in clays can change to a great extent, thus allowing access of polymer precursors or polymer chains that are intercalated from solutions or melts.[8,9] The high mechanical moduli found in nylon- or epoxy-exfoliated montmorillonite has stimulated research on these clay nanocomposites.[10,11]

Intercalation and, in the extreme case, exfoliation cause micro- and macroscopic changes of the layered hosts. On the other hand, truly crystalline porous supports can be filled with polymers while retaining their connectivity and morphology. We study the interaction of polymers with microporous zeolites and mesoporous MCM hosts having pores of uniform sizes that are present throughout the rigid inorganic matrix. We envision the formation of a polymeric network fully penetrating the inorganic hosts such that complete entanglement results. The composites produced in this way are anticipated to exhibit high mechanical and chemical stability.

Zeolites are crystalline, porous metal oxides (classically tectoalumino silicates) whose framework consists of well-defined pores and channels with pore openings between 3 and 10 Å. These hosts are expected to provide extensive control over the structure of the occluded polymer and over the associated host−guest interactions. Zeolites have recently been used for the reinforcement of polymer fibers. Mechanical mixing of zeolites A and 13X with hydroxyl-terminated poly(dimethylsiloxane) that was subsequently end-linked into elastomeric networks showed an increase in the ultimate strength of the composites. However, penetration of the polymers into the zeolite hosts and mixing on a molecular level had not been achieved.[12]

Bulk composites were prepared by imbibition of zeolite 13X with liquid styrene[13] or ethyl acrylate monomer[14] containing benzoyl peroxide initiator. Subsequent polymerization resulted in blends of 50/50 wt % polymer/zeolite. It was suggested that part of the polymers were incorporated into the zeolite pore system. This was concluded from slight line broadening in ^{13}C solid-state NMR spectra and an additional line in small-angle X-ray scattering (SAXS). The disappearance of a glass transition effect after solvent extraction of most of the bulk polymer in the composites located at the external surface of the zeolites was taken as a further indication. Similar experiments were performed with polystyrene in mesoporous MCM-41 with 28 Å diameter pores and in silica gel nanotubes with pores of 200−800 Å diameter.[15] A variety of zeolites have also been added in small amounts to aqueous solution of phenol and formaldehyde and subjected to thermal polymerization.[16] A strong increase in flexural strength of the composites containing zeolites suggested a partial polycondensation within their inner cavities.

Some of us have recently demonstrated the possibility of creating "molecular wires" through the templating action of zeolite hosts by aligning and connecting precursor molecules in the pores.[17] For example, monomers such as pyrrole,[18] anilin,[19] and thiophene[20] were adsorbed into zeolite channels and oxidatively polymerized. Polyacrylonitrile was formed in the channels of large-pore zeolites by radical polymerization of preadsorbed acrylonitrile.[21] The polymer was pyrolyzed to prepare conducting carbon filaments encapsulated in the zeolite host.[22] This work was extended by Mallouk et al. who used zeolites as templates for the formation of microporous polymers by dissolving the zeolitic support after polymer formation in the channels.[23a] Similarly, mesoporous MCM-41 acted as a mold in the formation of long polymer strands with a width of 20 Å.[23b]

The discovery of the M41S family by Mobil researchers in 1992[24] opened the possibility to study occluded polymers in defined pores exceeding the diameter of those found in zeolites. MCM-41 (hexagonal) and MCM-48 (cubic) are silicates or aluminosilicates with ordered pores. The choice of a surfactant "template" during synthesis determines the dimensions of these pores which can vary between 15 and 100 Å or even between 70 and 300 Å when block copolymers are used.[25] A review describing inclusion chemistry in MCM materials will soon be published.[26] Polymerization reactions of aniline and acrylonitrile in the hexagonal member of this family, MCM-41, have been reported recently by Wu and Bein.[27] The resulting polyaniline was present in its conductive form, while the included polyacrylonitrile could be pyrolized to produce conducting carbon filaments. Llewellyn et al.[28] used MCM-41 of two different pore sizes, 25 and 40 Å diameter, to study the polymerization of styrene, vinyl acetate (VA), and methyl methacrylate. The authors avoided polymer deposition on the outside of the MCM host by introducing the monomers from the gas phase. In these systems, the chain length of encapsulated PMMA increased with decreasing pore diameter. In a related study Aida et

(8) Giannelis, E. P. *Adv. Mater.* **1996**, *8*, 29.
(9) Krishnamoorti, R.; Vaia, R. A.; Giannelis, E. P. *Chem. Mater.* **1996**, *8*, 1728.
(10) Kojima, Y.; Usuki, A.; Kawasumi, M.; Okada, A.; Fukushima, Y.; Kurauchi, T.; Kamigaito, O. *J. Mater. Res.* **1993**, *8*, 1185.
(11) Lant, T.; Kaviratna, P. D.; Pinnavaia, T. J. *Chem. Mater.* **1995**, *7*, 2144.
(12) Wen, J.; Mark, J. E. *J. Mater. Sci.* **1994**, *29*, 499.
(13) Frisch, H. L.; Xue, Y. *J. Polym. Sci. A: Polym. Chem.* **1995**, *33*, 1979.
(14) Frisch, H. L.; Maaref, S.; Xue, Y.; Beaucage, G.; Pu, Z.; Mark, J. E. *J. Polym. Sci. Polym. Chem. Ed.* **1996**, *34*, 673.
(15) Frisch, H. L.; West, J. M.; Göltner, Ch. G.; Attard, G. S. *J. Polym. Sci. A: Polym. Chem.* **1996**, *34*, 1823.
(16) Kowalek, S.; Pawlowska, M.; Szuba, D. *J. Mater. Sci. Lett.* **1993**, *12*, 661.
(17) Bein, T. *Recent Advances and New Horizons in Zeolite Science and Technology*, Studies in Surface Science and Catalysis; Elsevier: Amsterdam, 1996; Vol. 102, p 295.
(18) Bein, T.; Enzel, P. *Angew. Chem., Int. Ed. Engl.* **1989**, *28*, 1692.
(19) Enzel, P.; Bein, T. *J. Phys. Chem.* **1989**, *93*, 6270.
(20) Enzel, P.; Bein, T. *J. Chem. Soc., Chem. Commun.* **1989**, 1326.
(21) Enzel, P.; Bein, T. *Chem. Mater.* **1992**, *4*, 819.
(22) Esnouf, S.; Beuneu, F.; Enzel, P.; Bein, T. *Phys. Rev. B.* **1997**, *56*, 12899.
(23) (a) Johnson, S. A.; Brigham, E. S.; Ollivier, P. J.; Mallouk, T. E. *Chem. Mater.* **1997**, *9*, 2448. (b) Johnson, S. A.; Khushalani, D.; Coombs, N.; Mallouk, T. E.; Ozin, G. A. *J. Mater. Chem.* **1998**, *8*, 13.
(24) Kresge, C. T.; Leonowicz, M. E.; Roth, W. J.; Vartuli, J. C.; Beck, J. S. *Nature* **1992**, *359*, 710.
(25) Zhao, D.; Feng, J.; Huo, Q.; Melosh, N.; Fredrickson, G. H.; Chmelka, B. F.; Stucky, G. D. *Science* **1998**, *279*, 548.
(26) Moller, K.; Bein, T. *Chem. Mater.* In press.
(27) (a)Wu, C.-G.; Bein, T. *Science* **1994**, *264*, 1757. (b) Wu, C.-G.; Bein, T. *Science* **1994**, *266*, 1013.
(28) Llewellyn, P. L.; Ciesla, U.; Decher, H.; Stadler, R.; Schüth, F.; Unger, K. K. *Zeolites and Related Microporous Materials: State of the Art*; Weitkamp, J., Karge, H. G., Pfeifer, H., Hölderich, W., Eds.; Studies in Surface Science and Catalysis; Elsevier: Amsterdam, 1994; Vol. 84, p 2013.

al.[29] polymerized PMMA in MCM-41 having 27-Å pores. They demonstrated that PMMA grown in the MCM host exceeded the bulk molecular weight by an oder of magnitude. The molecular weight could also be controlled by the stoichiometry of monomer to initiator.

This paper describes a comparative study on the polymerization of MMA in the internal cavities and channels in microporous as well as mesoporous hosts. We take advantage of the large inner surface of the porous hosts to achieve significant adsorption of the monomer and subsequent entanglement between the organic and inorganic phases in the resulting composites. Methyl methacrylate is introduced via gas-phase adsorption into the pore system of microporous zeolites with pore diameters between 5.1 and 7.6 Å, as well as in mesoporous MCM structures with pore openings between 30 and 35 Å. Polymerization is induced by benzoyl peroxide during thermal treatment. This synthesis route essentially eliminates deposition of bulk polymers on the outside of the inorganic matrix. Thus, we can study the polymerization in the internal pores and channels without the need for difficult extraction procedures. It will be demonstrated that the physical properties of the occluded polymers in our composites change significantly compared to bulk materials.

Experimental Section

(a) Preparation of Filler Materials. The following commercial zeolites were used: Faujasites NaY (PQ Corporation) and NaX (UOP), Mordenite (UOP), and H-ZSM-5 (UOP, Si:Al = 38:1) as well as fumed silica (CAB-O-SIL EH-5). All zeolite samples were calcined at 400 °C for 12 h in flowing oxygen with a heating rate of 2 °C/min. Colloidal zeolite beta (ca. 80 nm diameter) was prepared by following published procedures[30] and was calcined at 550 °C in air for 12 h.

MCM-41 was synthesized by following a room-temperature procedure described by Anderson et al.[31] Water (13.64) g and methanol 4.90 g were combined with 0.13 mL of 50 wt % aqueous NaOH solution (1.14 mmol) to result in a solution with a pH of 12.7. Subsequently, 1.408 g of cetyltrimethylammonium chloride (C_{16}TACl, 25% in water, Aldrich; 1.1 mmol) and 1.25 mL of tetramethoxysilane (TMOS, Aldrich; 8.47 mmol) were added under stirring. The final molar ratio was TMOS:C_{16}TACl:H_2O:MeOH = 1:0.13:97:18. A thick milky suspension formed within a minute, which was further stirred for 15 min and left at room temperature for 3−24 h. Filtration was followed by prolonged washing with water and drying at 70 °C. The removal of the surfactant was achieved by heating in air at 2 °C/min to 550 °C where the temperature was kept for 6 h.

The synthesis of the cubic member of the family of mesoporous M41S materials, named MCM-48, has been described.[32] We adapted a procedure reported by Schmidt et al.[33] A basic solution of pH 11.5 was prepared by dissolving 0.67 g of NaOH in 17 g of water. Tetraethyl orthosilicate (7.22 g, 98%, Aldrich) was added under stirring. After 5 min this solution was combined with 27.8 g of the template C_{16}TACl (25% in water) and was further stirred for 15 min. The final molar ratio was TEOS:Na_2O:C_{16}TACL:H_2O = 1:0.24:0.63:60.76. The white suspension was heated at 100 °C for 72 h in an autoclave. The resulting powder was washed until free of surfactant bubbles and dried at 70 °C. Template removal was performed by heating in a nitrogen flow at a rate of 2 °C/min to 540 °C. After 12 h at 540 °C the flow was switched to air, and the sample was kept at this temperature for another 6 h.

(b) Adsorption and Polymerization. Monomer adsorption of methyl methacrylate (MMA, 98%, Aldrich) into the porous supports was performed using the following procedure: About 1 g of the dry micro- or mesoporous material was evacuated on a vacuum line in a vertical tube reactor to a dynamic vacuum of less than 3×10^{-4} Torr while being heated at 200 °C for 12 h. In a second glass reactor MMA was frozen with liquid nitrogen, evacuated, and thawed again for three cycles. After the porous supports were cooled to room temperature, the reactors were separated from the pumps and the samples were exposed to MMA vapor under stirring for 1−2 h. Subsequently they were transferred into a nitrogen-filled glovebox and mixed with about 10 mg of benzoyl peroxide (99%, Aldrich). The closed containers were heated to 70 °C for 1−3 days. Subsequent heating to 120 °C for at least 2 h followed by evacuation at this temperature for 18 h resulted in the final composite.

(c) Sample Characterization. FTIR spectra (Mattson Instruments, Polaris; DTGS detector, 128 scans, 4 cm^{-1} resolution) were taken at every step during the reactions described above. A small amount of dry sample powder was spread between two KBr plates in a glovebox, sealed with vacuum grease, and immediately transferred into the nitrogen-purged chamber of the FTIR.

Surface areas before and after polymerization were determined from nitrogen adsorption/desorption isotherms collected at 77 K with a Coulter Omnisorp 100 instrument using static sampling. The samples were outgassed prior to adsorption at 120 °C for 18 h on a high-vacuum line. Micropore volume was determined from T-plots, while the pore volume of the mesoporous materials was calculated from the adsorbed nitrogen after complete pore condensation using the ratio of the densities of liquid and gaseous nitrogen (pore volume = mL/g adsorbed nitrogen (STP) × 0.001548).

Gravimetric determination of the entrapped amount of PMMA was performed on a DuPont TGA 951 thermal analyzer operated with a TA Instruments 2000 interface. About 10−20 mg of sample was heated at 2 °C/min to 600 °C in a stream of oxygen.

X-ray diffraction was performed on a Scintag XDS 2000 instrument equipped with a liquid nitrogen cooled germanium detector. Transmission electron micrographs of specimens (dispersed in ethanol by sonication) were taken with a JEOL FX-2000 microscope operated at 200 kV. Small droplets of these dispersions were evaporated on holey carbon grids.

Scanning electron microscopy images were taken with a Philips ElectroScan on powders dispersed in ethanol and dropped onto carbon studs. The samples were gold coated.

The glass transition temperature (T_g) was measured with a DSC 2910 differential scanning calorimeter from Thermal Instruments. Three to 15 mg samples were placed in covered aluminum pans, and the T_g was measured with a heating rate of 10 °C/min under nitrogen flow to 200 °C. Prior to the start of measurements, samples were kept at 70 °C for 20 min to desorb surface water.

Results and Discussion

Adsorption of MMA into Faujasites. Zeolites NaY and NaX belong to the family of faujasites which feature

(29) Ng, S. M.; Ogino, S.; Aida, T.; Koyano, K. A.; Tatsumi, T. *Macromol. Rapid Commun.* **1997**, *18*, 991.

(30) Van der Waal, J. C.; Rigutto, M. S.; van Bekkum, H. *J. Chem. Soc., Chem. Commun.* **1994**, 1241.

(31) Anderson, M. T.; Martin, J. F.; Odinek, J.; Newcomer, P. *Access in Nanoporous Materials*; Pinnavaia, T. J., Thorpe, M. F., Eds.; Plenum Press: New York, 1995; p 29.

(32) (a) Beck, J. S.; Vartuli, J. C.; Roth, W. J.; Leonowicz, M. E.; Kresge, C. T.; Schmitt, K. D.; Chu, C. T.−W.; Olson, D. H.; Sheppard, E. W.; McCullen, S. B.; Higgins, J. B.; Schlenker, J. L. *J. Am. Chem. Soc.* **1992**, *114*, 4, 10834. (b) Vartuli, J. C.; Schmitt, K. D.; Kresge, C. T.; Roth, W. J.; Leonowicz, M. E.; McCullen, S. B.; Hellring, S. D.; Beck, J. S.; Schlencker, J. L.; Olson, D. H.; Sheppard, E. W. *Chem. Mater.* **1994**, *6*, 2317. (c) Monnier, A.; Schüth, F.; Huo, Q.; Kumar, D.; Margolese, D.; Maxwell, R. S.; Stucky, G. D.; Krishnamurty, M.; Petroff, P.; Firouzi, A.; Janicke, M.; Chmelka, B. F. *Science* **1993**, *261*, 1299.

(33) Schmidt, R.; Stöcker, M.; Akporiaye, D.; Heggelund Torstad, E.; Olsen, A. *Microporous Mater.* **1995**, *5*, 1.

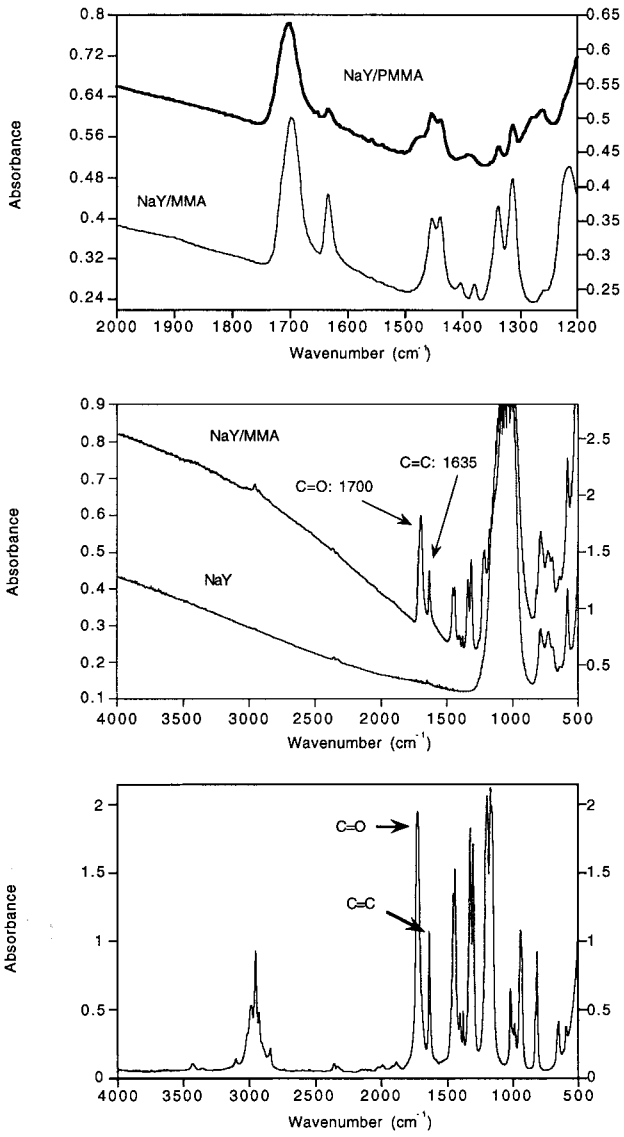

Figure 1. Transmission FTIR spectra of (bottom) liquid MMA, (middle) dehydrated zeolite NaY powder and NaY loaded with MMA, and (top) MMA in NaY before and after polymerization.

a three- dimensional channel system with pore openings constructed of twelve Si/AlO_4 units resulting in a 7.5-Å free pore diameter. Their major cavity, the supercage, is 13 Å in diameter. This crystalline channel system allows for easy access of molecular MMA having a maximum width of ca. 4.5 Å. The adsorption process can clearly be observed with infrared spectroscopy. The MMA monomer shows a very strong C═O ester carbonyl stretch vibration at 1726 cm^{-1} and a C═C stretch vibration at 1639 cm^{-1} as seen in Figure 1 (bottom). The zeolite hosts have only strong absorption bands between 800 and 1200 cm^{-1} resulting from their lattice vibrations, as shown in Figure 1 (middle). Most zeolites contain considerable amounts of water in their cages when not dehydrated. Our pretreatment results in completely dry powders, as evident from the absence of H_2O vibrations at 1640 cm^{-1} as well as the absence of the broad absorption around 3500 cm^{-1}. After adsorption of MMA into zeolite NaY, the two characteristic C═O and C═C bands of MMA are easily recognized (Figure 1, middle). The intensity of the C═O vibration relative to the Si−O band can be taken as a semiquantitative measure for the MMA amount adsorbed. It is remarkable that the C═O vibration is shifted to a much lower energy (1700 cm^{-1}) compared to the pure compound (1726 cm^{-1}) when MMA is absorbed in the zeolite host. A similar effect has been described by King et al. upon introduction of MMA into porous silica glass. They noted a shoulder at 1699 cm^{-1} within the major C═O peak, which was positioned at 1723 cm^{-1}.[3] They explained this shoulder as resulting from the formation of a hydrogen bond between some of the carbonyl oxygens and the (limited number of) acidic silanol groups of the support. Faujasites contain Lewis acid sites in the form of extra-framework cations residing in the supercages. In previous studies we have observed strong interactions between these cations and carbonyl ligands in metal carbonyl complexes resulting in shifts and splitting of C═O stretching vibrations.[34] In our present study we find shifted, but symmetric C═O bands indicating interaction of all MMA monomers with the Lewis-acid sites in the zeolite Y cages. Adsorption of MMA also shifts the $-C{=}CH_2$ frequencies at 1302 and 1325 cm^{-1} to 1312 and 1339 cm^{-1}. We also adsorbed MMA into dealuminated SiY which is devoid of cations in its inner cavities. Here, the C═O stretch vibration is found at 1733 cm^{-1}, confirming the sensitivity of MMA toward intrazeolite cations.

Polymerization of the intrazeolite MMA is observed through spectral changes as shown in Figure 1 (top). The MMA vibrations are shown here before polymerization (expanded region from Figure 1, middle) and after the monomer has reacted for 2.5 days at 70 °C with an additional heating to 120 °C for 1 h under vacuum. Most striking is a strong reduction of the C═C mode at 1635 cm^{-1} which is accompanied by a strong decrease of the bands at 1313 and 1339 cm^{-1}. Simultaneously, a band at 1388 cm^{-1} develops; the latter mode was assigned by Willis et al. to a (C−H) bending vibration of the methyl group in PMMA.[35] Additionally, a shoulder forms at 1484 cm^{-1} which was assigned by the same authors to a (C−H) bending vibration of the methylene group but is claimed to be a C−H bending vibration in $C{-}CH_3$ by Schneider et al.[36] We favor the former interpretation because this band arises upon reduction of the C═C double bond intensity. The strong bands at 1437 and 1449 cm^{-1} remain nearly unchanged during polymerization. This is plausible because they originate from $O{-}CH_3$ bending vibrations (the band at 1449 cm^{-1} has additional components of CH_2 and $C{-}CH_3$ bending modes) which should not be affected much during reaction. The C═O vibration remains largely unchanged upon polymerization, at 1706 cm^{-1}, but shifts to 1726 cm^{-1} upon adsorption of H_2O. This is in line with the suggested interaction of the intrazeolite MMA with surface acid sites that is reduced by competition with water molecules.

Infrared spectroscopy suggests that a large amount of MMA has interacted with the zeolite support, but it

(34) (a) Bein, T.; McLain, S. J.; Corbin, D. R.; Farlee, R. D.; Moller, K.; Stucky, G. D.; Woolery, G.; Sayers, D. *J. Am. Chem. Soc.* **1988**, *110*, 1801. (b) Özkar, S.; Ozin, G. A.; Moller, K.; Bein, T. *J. Am. Chem. Soc.* **1990**, *112*, 9575.

(35) Willis, H. A.; Zichy, V. J. I.; Hendra, P. J. *Polymer* **1966**, *7*, 387.

(36) Schneider, B.; Stokr, J.; Schmidt, P.; Mihailov, M.; Dirlikov, S.; Peeva, N. *Polymer* **1979**, *20*, 705.

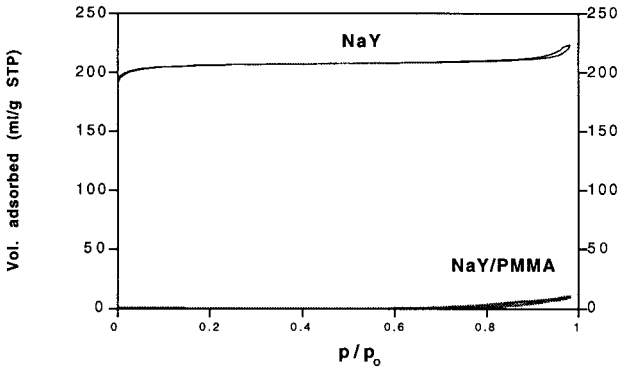

Figure 2. Nitrogen adsorption and desorption isotherms of (top trace) dehydrated zeolite NaY and (bottom trace) NaY after PMMA polymerization.

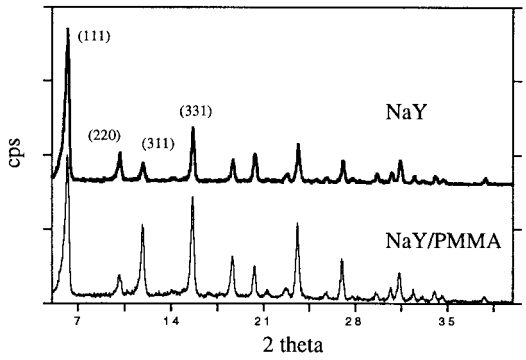

Figure 3. X-ray diffractograms of dehydrated zeolite NaY (top trace) and after PMMA polymerization (bottom trace).

cannot prove that the pores of the framework have been filled with the polymer. The microporosity of the zeolites was assessed through volumetric measurements of nitrogen uptake. A nitrogen adsorption/desorption isotherm of dehydrated NaY is shown in Figure 2 (top). Completely degassed zeolite NaY shows a type 1 isotherm, where filling of the micropores is achieved already at very low relative pressures, p/p_0, followed by surface adsorption of multilayers. The pore volume is calculated to be 0.32 mL of nitrogen/g of zeolite, which agrees well with literature values.[21] Strikingly, the zeolite micropores are completely filled with PMMA after polymerization, restricting any access of nitrogen into the pores of the zeolites. The adsorption isotherm now shows only a flat line for surface adsorption (Figure 2, bottom). The residual pore volume for different experiments varies between 0 and 0.037 mL/g after polymerization.

The effect of pore filling can also be seen from TGA measurements. Sample loading onto the balance arm exposes the zeolite powder to air. Previously dry zeolites take up water spontaneously during this process, resulting in an initial increase in weight and a subsequent water desorption of more than 20 wt %. This process is largely completed at 200 °C. A polymer containing sample, however, never shows an initial weight increase but only a weight loss of, at most ,4 wt %. Combustion of the organic content culminates at 285 °C while heating in an oxygen atmosphere. This decomposition temperature is close to the pyrolysis temperature of commercial bulk PMMA at 277 °C. Residue-free zeolite (as indicated by FTIR) is obtained after heating to 500 °C, and the polymer content can be calculated from the weight loss. Between 15 and 22 wt % of PMMA loading is obtained, where the variations are mainly due to different loading procedures. The highest loadings were achieved through stirring of the adsorbent during MMA exposure. A loading of 22 wt % corresponds to 300 mg of MMA/g of zeolite. It was determined from sorption measurements that 1 g of NaY can take up 350 mg of water or 250 mg of benzene.[37] From this comparison the complete filling of the internal pores with MMA seems to be very likely.

To ensure the crystallinity of the zeolite lattice after adsorption and polymerization of MMA, X-ray diffraction measurements were performed. In Figure 3 we compare zeolite NaY before and after adsorption and polymerization of methyl methacrylate. All Bragg reflections are still present after the composite is formed, but the relative intensities have changed. Changes of peak intensities are commonly observed for zeolites when the pore content is changed, for example, on hydration of the pores or redistribution of cations.[38] We observe similar effects in silicalite (the siliceous form of ZSM-5)/PMMA composites, when the pores are occupied with the guest species. For example, when XRD patterns are recorded for silicalite still containing the template tetrapropylammonium in its channels, the (101), (200), and (020) reflections are less intense than the (501) reflection. However, when the template is removed through calcination, these relative intensities are reversed.[39] As soon as calcined silicalite is imbibed with MMA and polymerized, the same reversal of intensities is observed. This phenomenon strongly suggests the presence of PMMA in the cavities of zeolite Y and silicalite.

Adsorption of MMA into Other Microporous Supports. As discussed below, zeolites with different channel openings and connectivities were also studied as hosts. Another structure with pores consisting of 12-membered rings is zeolite beta. Here, the pores do not form cages as in zeolite Y but consist of interconnecting straight channels with openings of 7.6 × 6.4 and 5.5 × 5.5 Å. Nitrogen adsorption shows a void volume of 0.23 mL/g (see Table 1).

Zeolite mordenite also has parallel straight pores. One type consists of 12-membered rings of similar dimensions as in beta, e.g., 6.7 × 7.0 Å. The second eight-membered channel, with dimensions of 2.6 × 5.7 Å, is not accessible to MMA. The measured pore volume of 0.13 mL of N_2/g of zeolite mordenite is smaller than that of faujasites or beta.

ZSM-5 has an interconnecting channel structure with still smaller dimensions of 5.3 × 5.6 and 5.1 × 5.5 Å. The nitrogen pore volume was assessed to be 0.10 mL/g.

For comparison, we also studied fumed silica that provides a large surface area (380 m^2/g determined by the manufacturer; we measured 350 m^2/g).

Adsorption of MMA into all of the above microporous supports was successful. Strong IR bands with similar intensity as in NaY were found in zeolite beta (as would

(37) Breck, D. W. *Molecular Sieves*; R. Krieger Publishing Company: Malabar, FL,1984.

(38) Dai, P.-S. E.; Lunsford, J. H. *J. Catal.* **1980**, *64*, 173.
(39) Moller, K. Unpublished results.

Table 1: Physical Properties of Porous Supports before and after Adsorption with MMA

		surface are (m^2/g)		pore volume (mL/g)				
zeolites	pore size (Å)	before adsorption	after adsorption	before adsorption	after adsorption	wt % PMMA (max)	PMMA/ zeolite (g/g)	theor vol. of PMMA (mL/g)[a]
NaY/X	7.4			0.32	0	22	0.30	0.25
beta	7.6 × 6.4			0.23		10.4	0.12	0.10
	5.5 × 5.5							
MOR	6.7 × 7.0			0.13	0	11	0.13	0.10
ZSM-5	5.3 × 5.6			0.10	0.07	7.5	0.07	0.06
	5.1 × 5.5							
silica		350	126			5	0.07	0.06
MCM-41	ca. 30	1200	45	0.62	0.02	37	0.59	0.50
MCM-48	ca. 35	1173	0	0.92	0	45	0.82	0.68

[a] PMMA volume calculated assuming a bulk density of 1.18 g/mL.

be expected from their comparable void volumes). In mordenite and zeolite ZSM-5 the initially adsorbed amount (judging from the IR) was much smaller from the beginning and seemed smallest in fumed silica, as expected from the smaller pore volumes and surface areas. In all of these samples we could observe the above-mentioned downshift of the C═O stretch vibration upon adsorption of MMA, to ca. 1700 cm^{-1}. Only in ZSM-5 did the C═O mode remain at 1727 cm^{-1}. This position is similar to that of liquid MMA and is presumably due to the absence of extra-framework cations.

Polymerization was very limited in zeolite beta. IR spectroscopy shows only a small conversion to PMMA even after heating to 120 °C for 20 h. However, evacuation for several hours did not deplete the sample completely of MMA, and the polymer content was determined with TGA to be 10.4 wt %. This suggests a polymerization at the pore entrances effectively blocking residual MMA from desorption under vacuum. Stacking faults in the beta structure could have caused the limited degree of polymerization. Polymerization was also only partially successful in ZSM-5, probably due to the smaller pore openings, but it was possible in mordenite and silica. Upon conversion of MMA to PMMA in the above samples, we observed a shift of the C═O band from 1700 to 1730 cm^{-1}, the wavenumber of bulk PMMA. This blue shift can be explained with the loss of delocalization between the C═O and C═C double bonds upon polymerization. The magnitude of this blue shift is smaller in NaY (from 1700 to 1706 cm^{-1}) probably due to the stronger interaction of the charge-balancing sodium cations with the carbonyl groups.

Quantitative determinations of the organic fractions in these composites were performed on all samples using thermogravimetry. Only the weight loss during pyrolysis was taken into account, so as to exclude weight losses due to desorption of water or unreacted monomers (both processes are usually completed below 150−200 °C; weight losses were determined above 200 °C). A summary is given in Table 1. Typically, several samples of each composite were prepared, but only the results with the highest polymer loadings are listed here. It can be seen that the loading of PMMA decreases from 22 wt % for zeolite NaY to 11 wt % in mordenite, down to 7 wt % in ZSM-5, and it is smallest on fumed silica with 5 wt %. We calculated theoretical volumes for PMMA on the basis of these polymer loadings and the bulk density of PMMA. These volumes are listed in Table 1 and are compared to the pore volumes determined by nitrogen adsorption. After polymerization, no remaining pore volume is detected in zeolites NaY and mordenite. The calculated volume fraction of encapsulated PMMA relative to the zeolite free pore volume is 78% in NaY and 85% in mordenite, respectively.

The smallest relative amount of pore filling with polymer, 60%, is found in ZSM-5, a sample where polymerization was incomplete. Since very little reaction took place in ZSM-5 it is likely that penetration of the initiator or radicals into the pores was not effective. The small amount of polymer might have formed from acid-catalyzed reactions during heating with simultaneous desorption of the remaining MMA, resulting in a large residual pore volume of 70% of the original 0.10 mL/g. Additionally, molecular modeling of PMMA oligomers in the channels of ZSM-5 indicates a close contact of the polymer with the surrounding zeolite walls. This might cause too much strain on the polymer chains, another reason to suppress internal polymerization. The polymer content of 7 wt % translates into ca. 0.06 mL/g of PMMA, which exceeds the 0.03 mL/g that is inaccessible to nitrogen after reaction. Thus, part of the PMMA was likely deposited on the external surface. A similar situation is found with fumed silica. We included this material because it has a high surface area but does not provide structural pores. Thus, the PMMA in this composite will be deposited in interparticle voids and as a surface film. This sample then serves as a standard to estimate the ultimate polymer content formed on outer surfaces under our reaction conditions. We measured a broad pore size distribution of textural pores between 15 and 120 Å in this material before loading with polymer. Some PMMA is deposited in the smaller interparticle pores (with diameters up to ca. 40 Å), leaving some meso- and macropores (which account for ca. 260 m^2/g of the total 350 m^2/g surface area) open for adsorption of nitrogen. The total of 5 wt % PMMA in this silica composite is much smaller than the loading found in our porous zeolite samples. Since the external surface in zeolites is much smaller than their internal surface area and is only a fraction of that in fumed silica, it is likely that most of the PMMA resides within the internal channels in the zeolite composites.

Adsorption and Polymerization in Mesoporous Materials. Two different members of the mesoporous MCM family with pore sizes of ca. 30 Å were studied to compare the inclusion chemistry of MMA in microporous zeolites with that in mesoporous supports. The hexagonal MCM-41 was prepared by following a room-temperature procedure that results in the typical regular arrangement of the straight one-dimensional pores. Its X-ray diffraction patterns before and after calcina-

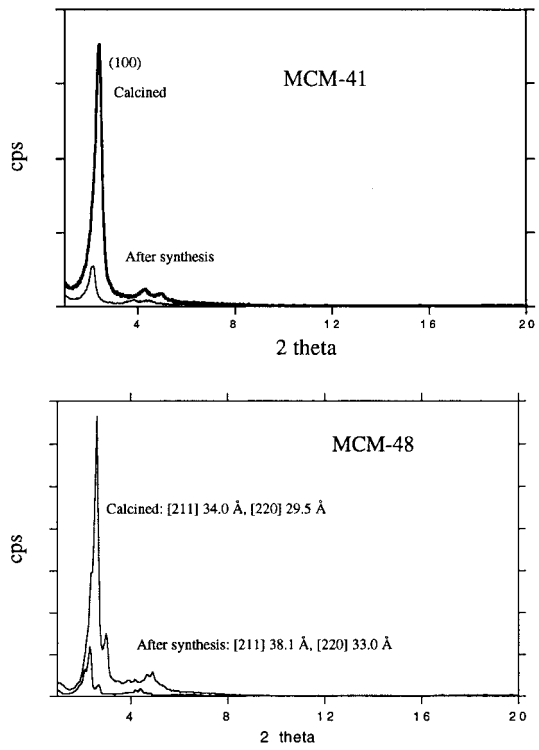

Figure 4. X-ray diffractograms of MCM-41 (top panel) and MCM-48 (bottom panel) hosts before (bottom trace) and after (top trace) calcination.

tion are shown in Figure 4a. The (100) Bragg reflection increases sharply in intensity upon removal of the hexadecyltrimethylammonium ion template. The *d* value decreases from 40.9 to 36.5 Å, as is commonly observed. Three additional small reflections ((110) = 20.6, (200) = 17.9, and (210) = 14.1 Å after calcination) are observed. Transmission electron micrographs show a pore diameter of ca. 25 Å and regular aligned pores throughout the entire volume of the particles (Figure 5a).

The cubic member of the MCM family, MCM-48, features pore sizes similar to those of MCM-41 when the same template is used during synthesis. However, the channels are twisted and accessible in all three directions. This host was included in our study because the three-dimensional arrangement of pores promises facile diffusion of monomer and initiator. After 3 days of hydrothermal synthesis at 110 °C, we obtained an XRD pattern with the diffraction peaks (211) and (220) at 41 and 38 Å before calcination, similar to the major peaks reported in the literature, as well as several other reported diffraction peaks (see Figure 4b).[32,33] We note that several slightly differing synthesis approaches were explored, e.g., tightly capping the reaction containers or leaving them loosely closed so as to allow for evaporation of the ethanol formed. High quality MCM-48 could only be obtained in autoclaves as described above. Electron microscopy on these materials reveals pore sizes similar to those of MCM-41, but here we can distinguish the characteristic pattern of the cubic (111) plane as well as the cubic (110) plane (see Figure 5b).

FTIR spectra of MMA adsorbed into the MCM-41 and MCM-48 materials show much larger peak intensities compared to the microporous samples (Figure 6, MCM-48 before and after polymerization). Upon adsorption we observe again a shift of the C=O vibration down to 1707 cm^{-1}. Simultaneously, the strong peak at 3743 cm^{-1} resulting from terminal surface hydroxyl groups in dry MCM-48 (not shown) is consumed and a broad peak due to hydrogen bonding develops around 3450 cm^{-1}. C−H bending vibrations of the monomer are also observed between 2848 and 2989 cm^{-1} in these samples. The former band has been assigned to a combination mode involving $O-CH_3$, a group that is also partially responsible for the bands at 2930, 2953, and 2996 cm^{-1}. The band at 2989 cm^{-1} also contains contributions from (CH_2) and (C−H) of the α-CH_3 stretch vibrations. The occurrence of the broad peak at 3450 cm^{-1} can therefore not be due to the possible hydrolysis of PMMA to methacrylic acid since the peak at 2848 cm^{-1} as well as those at 1443 and 1458 cm^{-1} prove the persistence of the $O-CH_3$ groups in methyl methacrylate. Furthermore, hydroxyl bands in carboxylic acid groups have

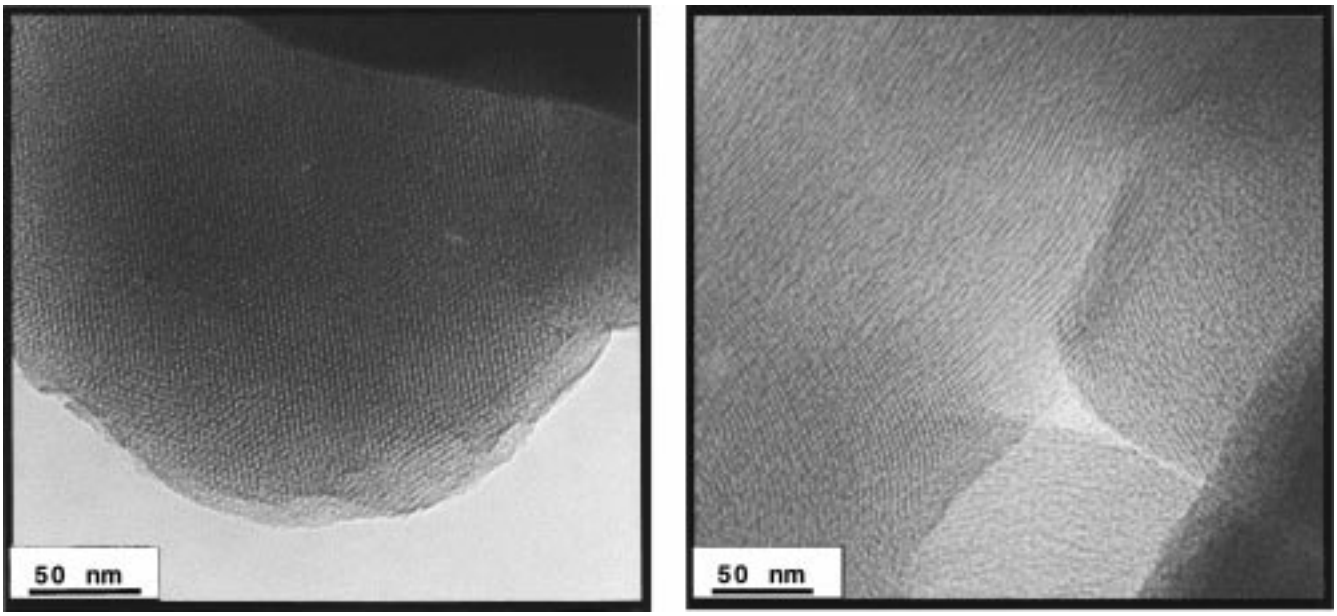

Figure 5. Transmission electron micrograph of (a, left) calcined MCM-41 and (b, right) calcined MCM-48.

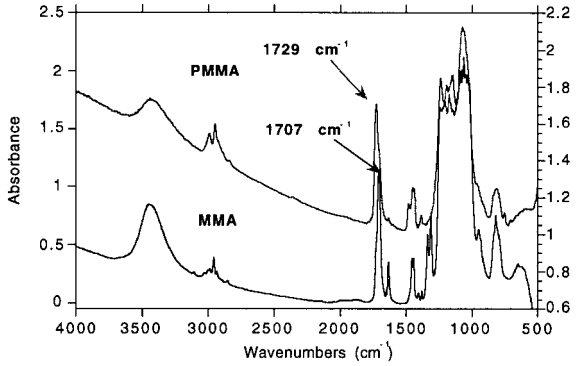

Figure 6. FTIR spectra of MMA-loaded MCM-48 before and after polymerization.

only been found at lower frequencies, between 3000 and 3200 cm^{-1}.[18,20] Upon polymerization of MMA, the carbonyl peak shifts again up to 1729 cm^{-1}, as was observed in most of the microporous zeolites, but a shoulder at 1706 cm^{-1} and very small traces of the C=C mode at 1639 cm^{-1} remain. A concomitant partial recovery of the terminal hydroxyl intensity is observed in MCM-41.

The high loading levels of PMMA in the mesoporous supports are reflected in their weight losses during oxidation in the TGA: up to 37 wt % PMMA is found in MCM-41 and even 45 wt % is found in MCM-48. Interestingly, the polymer is pyrolyzed over a narrower temperature range at much higher temperatures of ca. 350 °C in the latter samples (as well as in silica).

Nitrogen adsorption/desorption isotherms of calcined and polymer-filled MCM-41 and MCM-48 reveal slight differences between these mesoporous supports (Figure 7). Both materials exhibit type IV isotherms. However, filling of the large pores with nitrogen occurs over the relative pressure range of 0.18−0.28 in MCM-41, while this capillary condensation commences in a more narrow range (between 0.26 and 0.33) in MCM-48. Simultaneously, we observe a larger pore volume of 0.92 mL/g for MCM-48 as compared to 0.62 for MCM-41 while similar surface areas are determined (1173 and 1200 m^2/g). These findings indicate the existence of more uniform and larger pores in the cubic MCM-48.

We can estimate the pore dimensions from the unit cell formula for hexagonal lattices, where $a_0 = 2d_{100}/\sqrt{3}$. Assuming a wall thickness of ca. 10 Å, as is usually found in MCM synthesized in a similar procedure, pore dimensions are about 30 Å for the MCM-41. Somewhat larger pores must exist in MCM-48. Microporosity was not detected with T-plot analysis in either support. After adsorption and reaction of MMA within these pores, a residual BET area of 45 m^2/g is calculated in MCM-41. The adsorption step from the mesopores has disappeared, indicating their complete filling. No pore volume is detected for the MCM-48/PMMA composite.

Possible changes in morphology or microstructure in these samples were investigated with scanning and transmission electron microscopy. Figure 8 shows SEM scans of MCM-41 before and after polymerization. Particles of ca. 0.5 μm size with flaky morphology were found for this sample (Figure 8a). Some larger particles, as found in the MCM-41/PMMA sample (Figure 8b), were also found with the pure support; they do not

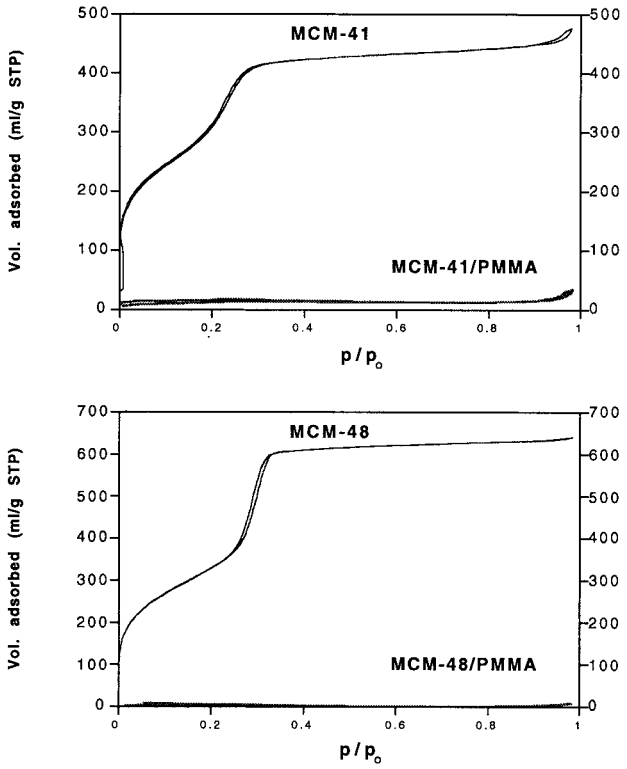

Figure 7. Nitrogen adsorption/desorption isotherms of MCM-41(top panel) and MCM-48 (bottom panel) in the dehydrated form (top trace) and after MMA polymerization (bottom trace).

indicate phase seggragation. A high-resolution electron microscopy image of MCM-41 after polymerization is shown in Figure 9. It reveals the same hexagonal pore structure of the host with the occluded PMMA as without. The well-defined crystal surfaces suggest that no enrichment of PMMA on the exterior of the crystals had occurred. We note that these specimens were the most stable to the electron beam exposure compared to MCM samples that lack the stabilizing effect of the acrylic glass within its pores.

Rather homogeneous, roundish particles sized 0.5−1 μm are obtained in the MCM-48 synthesis. As already mentioned for MCM-41, we do not see polymer accumulation on the outer surface when samples are compared before adsorption (Figure 10a) and after polymerization (Figure 10b).

Comparison of Micro- and Mesoporous Composites. In the following we summarize our results to demonstrate that filling of the pores with MMA/PMMA was accomplished in a variety of hosts. It was found that (a) the hydroxyl groups lining the pore walls as well as extraframework cations interact with the guest upon adsorption; (b) polymerization is only effective with pore openings adequate to allow penetration of the initiator; (c) lattice diffraction patterns change upon adsorption, indicating the presence of guest species; and (d) electron microscopy does not show any evidence of surface layers. Additionally, we show in Figure 11 how the host pore volume determines the amount of encapsulated PMMA. In Figure 11 the pore volumes of the hosts are presented in light patterns. The volumes for encapsulated PMMA were calculated using the polymer content and the density of bulk PMMA of 1.18 g/mL and are shown in dark patterns. The specific free pore volume of the host increases from ZSM-5 to MCM-48, and simultaneously

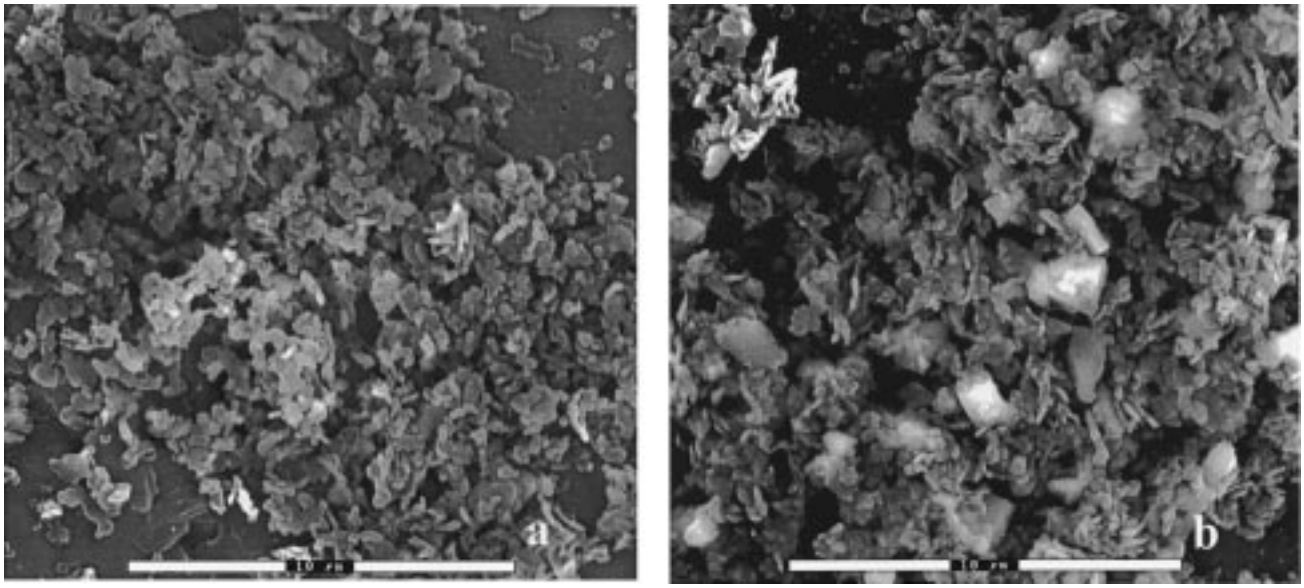

Figure 8. Scanning electron micrographs of MCM-41 (a) after template removal and (b) after MMA polymerization.

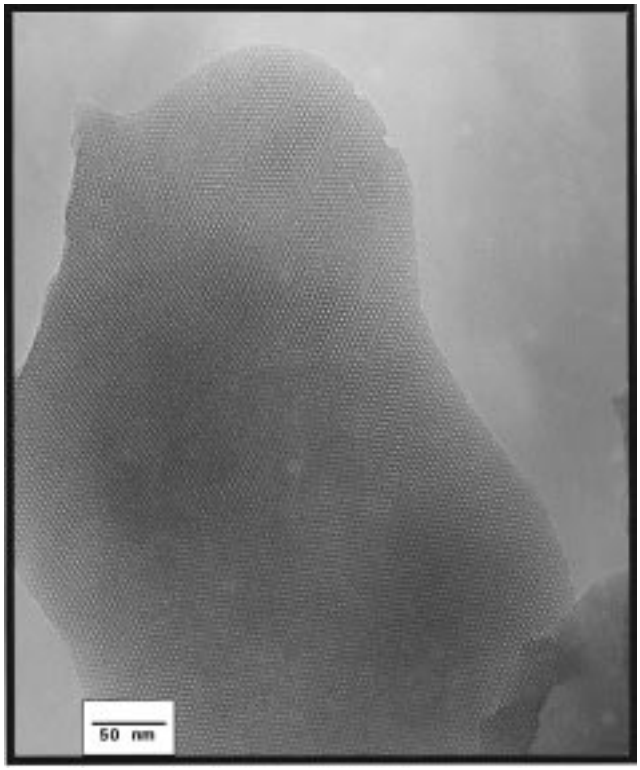

Figure 9. Transmission electron micrograph of MCM-41/PMMA.

the volume of encapsulated PMMA rises. The fraction of polymer-filled volume in the zeolites is smallest in ZSM-5 with 60% and higher in mordenite with 85% and in NaY with 78%. These values are only given to demonstrate the *minimum* amount of pore filling, assuming the validity of the above bulk density. However, it is difficult to estimate a realistic value for the density because the polymer is structured by the zeolite framework, which will have an effect on packing efficiency. On the basis of the molecular dimensions of MMA (approximately 4.5 × 6.8 Å), diffusion is possible throughout the larger channels in all the microporous zeolites. On the other hand, the polymeric chain has an estimated diameter (by molecular modeling) of at least 6.7 Å even when completely isotactic. Therefore, a close packing of more than one polymer strand is very unlikely in these channels, although the supercages of zeolite Y offer enough room for more than one chain segment. In other words, even if part of the PMMA resides as a thin film on the outer surface (which amounts to a very small fraction), more than the above-calculated volumes are probably filled with PMMA in these composites.

We propose that the formation of more densly packed polymer is likely within the larger pores of MCM materials. Several parallel polymer strands can fit into these channels. Within MCM-41, up to 81% of the free pore volume is occupied when bulk density is applied, while in MCM-48, where channels are interconnected and open in all three dimensions, pore filling up to 75% results. In summary, it is possible to obtain a formal pore filling of about 80% in all of the inorganic supports where polymerization is unrestricted.

Glass Transition Temperatures of Composites. The PMMA in the above composites is most likely confined in the form of polymer filaments with variable thickness according to the pore dimensions of the surrounding host. It is of interest to examine how the structural differences of these filaments relate to their physical properties. One feature characteristic of amorphous bulk polymers is their glass transition temperature, T_g. At this transition segmental motion and rotation about covalent bonds sets in. The glass transition of a commercial sample of PMMA (Polymer Products) was compared with those of the PMMA−zeolite composites (Figure 12). The commercial sample shows a T_g of 111 °C, which is intermediate between 105 °C for atactic PMMA[40] and 115 °C for syndiotactic PMMA[41] as reported in the literature. However, none of our microporous composites, including the fumed silica sample, showed an endothermic effect as would be expected for the onset of relaxation in PMMA. As an

(40) Seymor, R. B.; Carraher, C. E., Jr. *Polymer Chemistry: An Introduction*; Marcel Dekker: New York, 1988.
(41) *Handbook of Plastic, Elastomer and Composites*; Harper, C. A., Ed.; McGraw-Hill Inc.: New York, 1992.

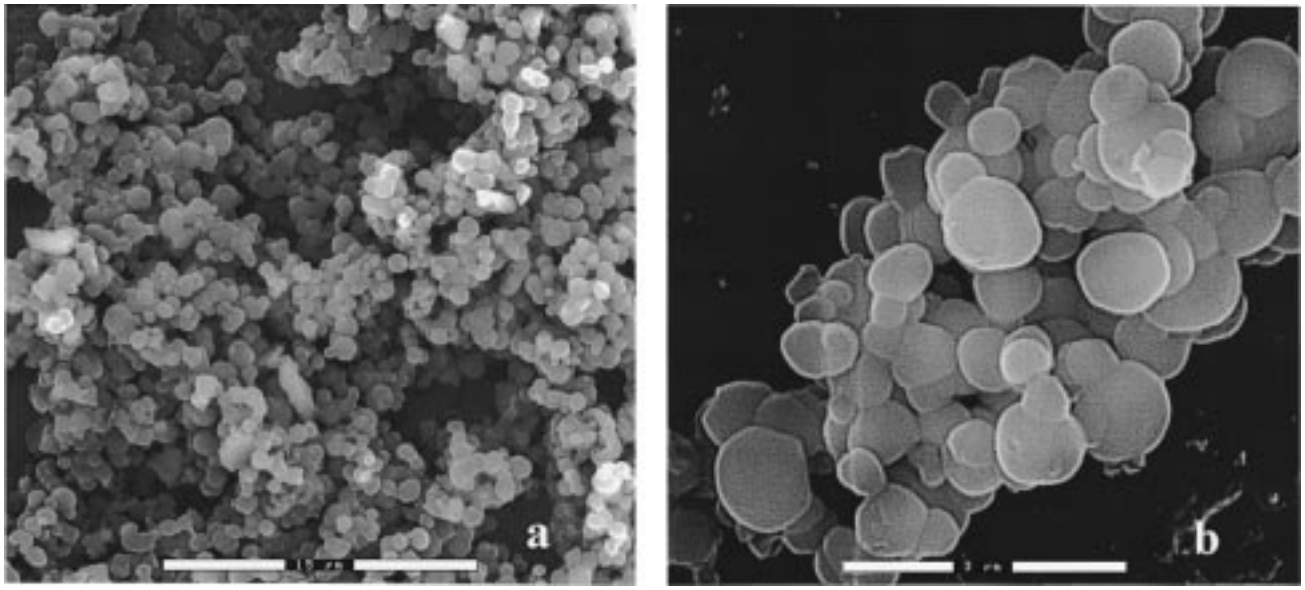

Figure 10. Scanning electron micrographs of MCM-48 (a) after template removal and (b) after MMA polymerization

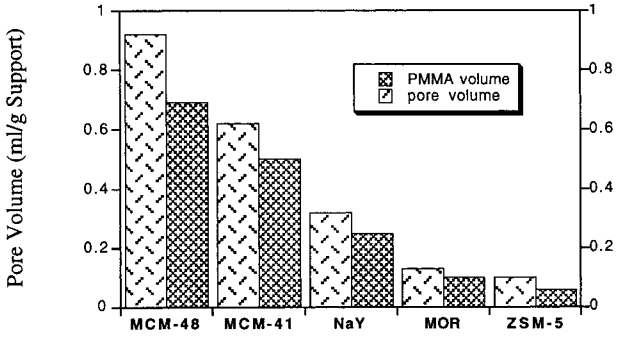

Figure 11. Degree of pore filling of various supports with PMMA. Light pattern, pore volumes of the empty hosts; dark pattern, volume of occluded PMMA, assuming a density of 1.18 g/mL for PMMA.

example, we show the DSC scan of a NaY/PMMA composite together with a scan of dry zeolite containing no polymer. This zeolite composite had the highest loading of PMMA of all microporous samples. However, the DSC scan of this composite is very similar to that of the zeolite powder itself. For comparison, a composite of MMA and zeolite NaY was prepared by imbibition such that excess PMMA has deposited on the outer surface of the zeolite, in addition to filling the pores. To achieve this, liquid MMA was added to dry zeolite powder in a dry nitrogen atmosphere until all zeolite was wetted. Polymerization was performed as before, which brought the PMMA content to 45 wt %, more than twice as much as in the composite prepared via gas-phase adsorption. For this sample, the DCS scan shows a glass transition at 122 °C, significantly higher than that of bulk PMMA (111 °C).

Compared to the zeolite hosts, a higher weight percentage of PMMA is occluded in MCM-41 (37 wt %) and MCM-48 (45 wt %). The PMMA content in the latter sample is close to that in zeolite NaY prepared by imbibition. However, even in these samples we could not detect a glass transition. Mixtures of dehydrated zeolites or MCM powders and commercial PMMA were prepared with a polymer content similar to that of the composite samples. These mixtures showed all readily observable glass transitions at temperatures between

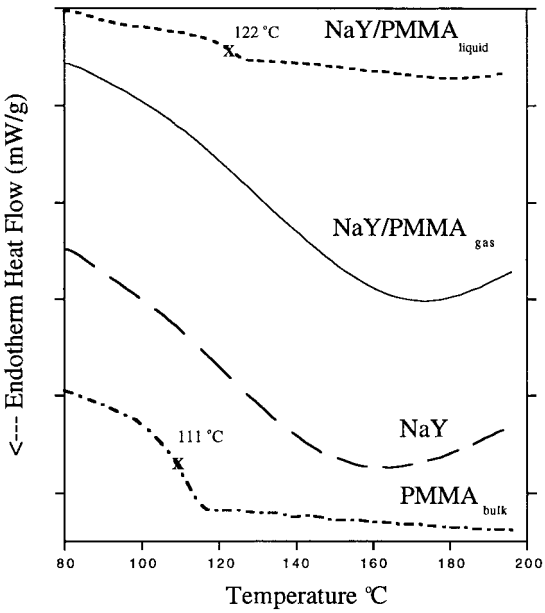

Figure 12. Differential scanning calorimetry of (from bottom to top) commercial bulk PMMA, dehydrated NaY powder, NaY after MMA polymerization (prepared via gas-phase adsorption; 22 wt % PMMA), and NaY/PMMA composite (prepared via imbibition; 45 wt % PMMA).

113 and 114 °C, even if the total amount of sample was reduced such that only 1 mg of PMMA was present.

In the following, we will put the above observations in perspective by comparing our results with those on related systems. In general, other authors observed a glass transition in composites whenever large amounts of bulk polymer were deposited on the surface of the fillers. A shift to a higher T_g (as we have found in the imbibed 45 wt % PMMA/zeolite composite) was described by Pu et al.[42] in 65/35 wt % PMMA/silica composites. The silica particles (of about 150 nm diameter) were treated with the silane-coupling agent 3-(trimethoxysilyl)propyl methacrylate. The glass tran-

(42) Pu, Z.; Mark, J. E.; Jethmalani, J. M.; Ford, W. T. *Chem. Mater.* **1997**, *9*, 2442.

sition shifted to higher temperatures with increasing amounts of filler and changed with the dispersion of filler in the organic matrix. Frisch et al.[15] found an increase of 13 °C when zeolite X was immersed to 50 wt % in cross-linked polystyrene (PS). A regular T_g was observed with the same polymer in a 70/30 wt % polymer/filler composite with mesoporous silica having comparatively larger pores of 28 Å or in an 80/20 wt % composite containing silica nanotubes with 200−8000 Å sized pores. The glass transition temperature was undetectable when the bulk polymer was extracted down to a 25/75 wt % composition with zeolite Y and with mesoporous silica filler. Only the large-pore nanotubes retained their glass transition. Similar observations were found for a poly(ethyl acrylate)/NaX zeolite system.[14] Again, no T_g was found as soon as the external phase of the polymer was extracted from the composite.

Wei et al.[43] prepared hybrid materials by copolymerization of styrene with 3-(trimethoxysilyl)propyl methacrylate that was subsequently hydrolyzed and cocondensed with TEOS in a sol−gel procedure to give monolithic glasses. While the organic copolymer alone showed a glass transition temperature close to that of PS, no T_g was found for the silica-containing hybrid materials with polymer contents up to 62 wt %. This was taken as an indication of a uniform mixture between the silica glass and the organic polymer. Giannelis et al.[44] could show that a physical mixture of polystyrene with a derivative of montmorillonite clay did show the usual T_g, but when the same amount of PS was intercalated into the galleries of the support, the glass transition disappeared.

In contrast, when Llewellyn et al.[28] prepared poly(vinyl acetate) (via gas-phase sorption of vinyl acetate) in two mesoporous MCM hosts with 25- and 40-Å pores (25−30% PVA) such that the majority of the polymer resides within the channels, they had indications for a weak glass transition. This event was shifted to higher temperatures in comparison to the bulk, by about 24 °C for the smaller and by 34 °C for the larger channel system. No reports were given for their PMMA composites. On the other hand, when silica with a mean pore size of 156 Å was immersed in MMA and polymerization was performed to result in a transparent monolith, a decrease in T_g of 15 °C compared to bulk PMMA was observed.[6]

Taking these reports together, it is obvious that at this point there are no clear conclusions to be drawn regarding the properties of polymers in nanocomposites. However, the major trend seems to be that when bulk polymer can be excluded by either dissolving thick layers or by avoiding its formation from the outset through gas-phase filling of internal pores, the surface interactions with the support become dominant and suppress the long-range motion of polymer strands.

There are several recent studies that focus on the behavior of thin polymer films at interfaces. For instance, it is well-known that the freezing temperature of liquids decreases with decreasing pore sizes. This was found for organic molecular liquids in porous silica glass with pore radii from 18 to 152 Å.[45] A similar trend was observed in controlled pore glasses with pores between 40 and 730 Å.[46]

In related model studies of confined systems, phase transitions in solid polymer films on surfaces were investigated. For example, thin polystyrene (PS) films with thicknesses between 45 and 835 Å were spin-coated on Si(111) substrates covered with a 15−25-Å oxide layer.[47] Contractions in film thickness at temperatures well below the glass transition temperature for bulk PS were observed during heating of samples with a 45−100-Å PS layer. Similarly, dewetting effects of PS on silicon below the bulk T_g were explained with a reduced transition temperature in confined films.[48] Studies on PMMA gave very different results: for thin films (75−570 Å) on silicon substrates, indications for an increase in T_g with decreasing film thickness were reported.[49] Similarly, an increase in the T_g of PMMA on oxidized silicon substrates with decreasing film thickness was observed.[50] However, when a film of gold was deposited on the silicon prior to PMMA, the T_g decreased with decreasing thickness. These differences were explained by a stronger interaction of PMMA with the silicon surface via hydrogen bonds which are not available on gold.

The importance of chemical interactions with the interface is further supported by Wallace et al.[51] They etched silicon surfaces and formed a monohydride layer before deposition of PS. Under these circumstances, no T_g could be measured with X-ray reflectivity up to 400 Å film thickness. The authors take this as a strong indication that adhesion to the surface is most important and that interface effects reach even further than model calculations have suggested.

In our PMMA/zeolite composites, the "film thickness" of PMMA in the internal pores will be much smaller than in most of the systems discussed above. Thus, we will have an even closer contact between surface and polymer because the polymer strands are completely sourrounded by inorganic pores of molecular diameters. The presence of strong surface interactions is supported by vibrational spectroscopy. In all cases, the methacrylate carbonyl mode is shifted relative to the bulk (up to 27 cm^{-1} in NaY). This strong interaction together with the prevailing one-dimensional confinement of the polymers might explain the nonexistence of a glass transition.

Conclusions

In conclusion, we have shown that it is possible to adsorb MMA from the gas phase into two- and three-dimensional channel systems with pores between 5.5 and 35 Å. Polymerization can be initiated with benzoyl

(43) Wei, Y.; Yang, D.; Tang, L.; Hutchins, M. *J. Mater. Res.* **1993**, *8*, 1143.
(44) Vaia, R. A.; Ishii, H.; Giannelis, E. P. *Chem. Mater.* **1993**, *5*, 1694.
(45) Zhang, J.; Liu, G.; Jonas, J. *J. Phys. Chem.* **1992**, *96*, 3478.
(46) Jackson, C. L.; McKenna, G. B. *J. Non-Cryst. Solids* **1991**, *131*, 221.
(47) Orts, W. J.; van Zanten, J. H.; Wu, W.; Satija, S. K. *Phys. Rev. Lett.* **1993**, *71*, 867.
(48) Reiter, G. *Macromolecules* **1994**, *27*, 3046.
(49) Wu, W.; van Zanten, J. H.; Orts, W. J. *Macromolecules* **1995**, *28*, 771.
(50) Keddie, J. L.; Jones, R. A. L.; Cory, R. A. *Faraday Discuss.* **1994**, *98*, 219.
(51) Wallace, W. E.; van Zanten, J. H.; Wu, W. L. *Phys. Rev. E* **1995**, *52*, R3329.

peroxide and propagated into the channels, affording radical chain growth, and almost complete conversion to polymer in the larger channel systems. Micropores as well as mesopores are effectively blocked for sorption of nitrogen or water after polymerization. The amount of the organic material in the nanocomposites together with volumetric data suggests that most of the pore volume is filled with PMMA. High surface area, nonporous silica composites were coated with much smaller polymer loading compared to the loadings in the porous materials. The absence of a glass transition event in the composites prepared via gas-phase adsorption is also taken as evidence for the incorporation of the polymer into the pores of the different supports and confirms strong polymer-host interactions at the nanometer scale.

Acknowledgment. The authors would like to thank Dr. Svetlana Mintova for providing the zeolite beta samples and for her help in obtaining the SEM images, and Dr. Said Mansur for performing transmission electron microscopy on our samples. Financial support for this work from the Bundesministerium für Bildung und Forschung (BMBF, Germany) is greatly acknowledged.

CM980020O